Accepted Manuscript

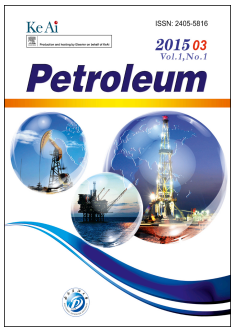

Velocity profiles description and shape factors inclusion in a hyperbolic, one-dimensional, transient two-fluid model for stratified and slug flow simulations in pipes

Arianna Bonzanini, Davide Picchi, Marco Ferrari, Pietro Poesio

PII: S2405-6561(17)30167-0

DOI: 10.1016/j.petlm.2018.03.005

Reference: PETLM 197

To appear in: *Petroleum*

Received Date: 16 August 2017

Accepted Date: 8 March 2018

Please cite this article as: A. Bonzanini, D. Picchi, M. Ferrari, P. Poesio, Velocity profiles description and shape factors inclusion in a hyperbolic, one-dimensional, transient two-fluid model for stratified and slug flow simulations in pipes, *Petroleum* (2018), doi: 10.1016/j.petlm.2018.03.005.

Velocity profiles description and shape factors inclusion in a hyperbolic, one-dimensional, transient two-fluid model for stratified and slug flow simulations in pipes

Arianna Bonzanini[a], Davide Picchi[b], Marco Ferrari[c], Pietro Poesio[a,*]

[a] *Università degli Studi di Brescia, Dipartimento di Ingegneria Meccanica ed Industriale, Via Branze, 38, 25123 Brescia, Italy*
[b] *Stanford University, Energy Resources Engineering, Stanford 94305, CA, United States.*
[c] *Politecnico di Milano, PoliMi, Department of Mathematics, 20133 Milan, Italy*

Abstract

In a previous work it has been shown that a one-dimensional, hyperbolic, transient five equations two-fluid model is able to numerically describe stratified, wavy, and slug flow in horizontal and near-horizontal pipes. Slug statistical characteristics can be numerically predicted with results in good agreement with experimental data and well-known empirical relations. In this model some approximated and simplified assumptions are adopted to describe shear stresses at wall and at phase interface.

In this paper, we focus on the possibility to account for the cross sectional flow by inserting shape factors into the momentum balance equations of the aforementioned model. Velocity profiles are obtained by a pre-integrated model and they are computed at each time step and at each computational cell. Once that the velocity profiles are known, the obtained shape factors are inserted in the numerical resolution. In this way it is possible to recover part of the information lost due to the one-dimensional flow description.

Velocity profiles computed in stratified conditions are compared against experimental profiles measured by PIV technique; a method to compute the velocity profile during slug initiation and growth has been developed and the computed velocity distribution in the liquid phase was compared against the one-seventh power law.

Keywords: multi-phase pipeline transport, oil&gas, hyperbolic two-fluid model, velocity profiles, shape factors

1. Introduction

Stratified and slug flows are two-phase flow regimes frequently encountered in transport of oil and gas in pipelines. In the past decades, the interest in the numerical

*Corresponding author
Email addresses: a.bonzanini001@unibs.it (Arianna Bonzanini), dpicchi@stanford.edu (Davide Picchi), marco2.ferrari@polimi.it (Marco Ferrari), pietro.poesio@unibs.it (Pietro Poesio)

description of these flow regimes has significantly increased, aiming at obtaining predictions about the behaviour of the fluids employed in petroleum transport pipelines, chemical and nuclear industries, and buoyancy driven fermentation devices.

Mathematical models adopted to describe flow behaviour call for closure relations for shear stresses at interface and at wall. Interfacial and wall shear stresses are related via the velocity distribution and, therefore, the cross-sectional flow description is required to obtain consistent modelling. Two-dimensional and three-dimensional models allow to describe this multi-dimensional relation but they are computationally expensive and require too long computational times. Then, to keep reasonable simulation times, Authors usually adopt one-dimensional averaged models, as the two-fluid one, see [1], [2]. In this model, closure relations for shear stresses are formulated in a simplified manner, losing the possibility to describe multi-dimensional effects, such as the connection between interfacial and wall shear stresses itself, see [3]. To solve the issue of computational speed versus physical consistency, the cross-sectional velocity profiles can be described by a pre-integrated model, which leads to a consistent set of near-algebraic friction models suitable for one-dimensional two-phase flow simulations, as showed by Biberg [4].

In the present work, to compute transient velocity profiles in slug flow conditions (or when a slug arises from stratified flow), we aim at introducing the velocity profiles shape description in the one-dimensional, transient, hyperbolic five-equation two-fluid model developed by Ferrari et al. [5]. They showed that this model has some great advantages if compared to the traditional four-equation two-fluid model: thanks to the addition of an equation that describes the advection of the gas volume fraction, it is always hyperbolic without the introduction of viscous terms often difficult to be numerically solved; however, surface tension effects are recovered through the solution of a pressure relaxation process. Moreover, Ferrari et al. [5] demonstrated that the five-equation model, by the introduction of ad-hoc flow regime transition criterion in the numerical solver, allows to capture very well slug formation and development, only adopting a flow description consistent with stratified conditions. Flow pattern transitions and slug flow characteristics predicted by the numerical code developed by Ferrari et al. [5] are in great agreement with experimental data or empirical correlations. Nevertheless, they assumed that the profiles coefficients were unitary ($\gamma_l = \gamma_g = 1$), representing a completely flat profile. The profiles coefficients are correction factors adopted to describe the curvature of the velocity profile, since the latter is not constant over the entire cross section and, for turbulent flows, the profile coefficient is slightly above one. To account for the cross-sectional velocity, we need to modify the five-equation system eigenstructure proposed in [5], inserting the γ factors in the modelisation; then, we adopt the pre-integrated model developed by Biberg [4], to describe the shear stresses at interface and at wall consistently with the modelling of the velocity profiles.

In this paper, the comparison of the computed velocity profiles in stratified conditions against the experimental ones measured by [6] will be reported, showing a fairly good agreement; then, results in slug flow will be presented, showing how to describe numerically the velocity profiles during the transition from two-phase to single phase flow (which takes place during slug formation) and comparing the obtained velocity profiles against the one-seventh power law [7], [8].

2. Model

In this work, we adopt the one-dimensional, hyperbolic, transient, five-equation, two-fluid model proposed in [5], which is able to compute flow regimes transitions and slug flow characteristics.

The five-equation system by Ferrari et al. [5] is composed by the four-equation of the traditional two-fluid model, two mass and two momentum equations, one for each phase, and by a further equation, which represents the advection of the gas volume fraction. Phases are treated as compressible and the energy equations are disregarded. Thanks to the addition of the further equation, Eq. (1), the model becomes hyperbolic without the addition of viscous terms, which are usually hard to be solved numerically. However, surface tension effects are recovered by the source term in the right-hand side of the advection equation, which is solved through an instantaneous pressure relaxation process to ensures the pressure equilibrium at the interface between the two phases, see [5], [9] and [10].

In the present work, the first modification performed on the model consists in inserting the shape factors γ_g and γ_l, for gas and liquid phase, respectively, in the momentum balance equations, Eqs. (4) - (5); therefore, the five-equation system proposed in [5] is rewritten as

$$\frac{\partial \alpha_g}{\partial t} + u_i \frac{\partial \alpha_g}{\partial x} = r_p(p_{ig} - p_{il}), \tag{1}$$

$$\frac{\partial (\alpha_g \rho_g)}{\partial t} + \frac{\partial (\alpha_g \rho_g u_g)}{\partial x} = 0, \tag{2}$$

$$\frac{\partial (\alpha_l \rho_l)}{\partial t} + \frac{\partial (\alpha_l \rho_l u_l)}{\partial x} = 0, \tag{3}$$

$$\begin{aligned}\frac{\partial (\alpha_g \rho_g u_g)}{\partial t} + \frac{\partial (\gamma_g \alpha_g \rho_g u_g^2)}{\partial x} + \alpha_g \frac{\partial p_{ig}}{\partial x} + \rho_g \alpha_g g \frac{\partial h}{\partial x} \cos(\theta) = \\ - \rho_g \alpha_g g \sin(\theta) - F_{wg} - F_i,\end{aligned} \tag{4}$$

$$\begin{aligned}\frac{\partial (\alpha_l \rho_l u_l)}{\partial t} + \frac{\partial (\gamma_l \alpha_l \rho_l u_l^2)}{\partial x} + \alpha_l \frac{\partial p_{il}}{\partial x} + \rho_l \alpha_l g \frac{\partial h}{\partial x} \cos(\theta) = \\ - \rho_l \alpha_l g \sin(\theta) - F_{wl} + F_i,\end{aligned} \tag{5}$$

where α is the volume fraction, ρ is density, u stands for phase velocity in the x direction and p for pressure; p_{ig} and p_{il} are gas and liquid interfacial pressures; θ is the inclination angle, see Fig. 1; the subscripts l and g stand for liquid and gas phase, respectively; interfacial variables have the subscript i and the subscript w indicates the wall; g is the acceleration due to gravity and h stands for the liquid height. The F terms stand for the frictional forces per unit volume and they need closure relations: Ferrari et al. [5] adopt the combination proposed by Issa and Kempf [1], where the Hagen-Poiseuille formulae are used for laminar flow and the Taitel and Dukler [11] correlations are adopted for turbulent flow, for gas-wall and interfacial friction factor, while the Kowalsky [12] model modified by Hand [13] is employed for the liquid-wall friction factor. In the present work, the formulation reported in Eq. (16) is adopted for the computation of gas-wall shear stresses, while liquid-wall and interfacial shear stresses are obtained following the model proposed by Biberg [4]. Friction factors are computed using the Colebrook-White

interpolation, Eq. (14). Finally, we adopt the same equation of state, which relates the pressure and density, employed by Ferrari et al [5].

The introduction of the shape factors in the model equations modifies the eigenstructure of the system; since the numerical resolution of the model is based on the Roe linearisation, see Section 3, the knowledge of the system eigenstructure is required. Thus, as first step of this work, the eigenvalues and eigenvectors of the five-equation system containing the shape factors were computed; we remark that, if the shape factors in the modified eigenstructure are set to one (as supposed in the previous work by Ferrari et al. [5]), the original version of the eigenstructure is recovered. However, despite these changes in the eigenstructure, the model keeps the hyperbolicity property. The comparison of the old eigenstructure against the new one including shape factors and a discussion on the hyperbolicity is reported in Appendix A.

The pre-integrated model proposed by Biberg [4] is adopted to compute the cross-sectional velocity profiles, which are required to obtain the shape factors, see [14], defined as

$$\gamma_j = \frac{1}{A_j v_j^2} \int v_j^2(y) dA, \tag{6}$$

where A_j represents the cross-section occupied by the phase j and v_j stands for the velocity distribution in the y direction, which is computed as proposed by Biberg [4]

$$v_j = \int \frac{\tau_{xy}}{\mu^t} dy. \tag{7}$$

In Eq. (7) τ_{xy} represents the shear stress distribution and μ^t is the eddy viscosity; this latter is computed in a rigorous mathematical way and an algebraic expression is obtained by the definition of the mixing length, which accounts for the non-constant shear stress distribution along the pipe cross section, and through the Prandtl mixing-length hypothesis.

Thanks to the algebraic expression of the eddy viscosity μ^t, Eq. (7) can be re-written as

$$v_j = sgn(\tau_{wj}) \frac{u^*}{\kappa} \Delta_j + C_j, \tag{8}$$

where Δ_j and C_j, whose formulation is reported in Appendix B, are functions of Y, the adimensional position along the pipe cross section, of R_j, the ratio between the shear stress at interface τ_i, and the one between phase j and the wall τ_{wj}

$$Y = \frac{y}{h}, \qquad R_j = \frac{\tau_i}{\tau_{wj}}, \tag{9}$$

and of K_j, a parameter accounting for the interface shape, which reads, respectively for gas and liquid phase,

$$K_g = \frac{8\nu_g}{|u_g - u_l|}, \quad K_l = 1, \tag{10}$$

in case of smooth interface, and

$$K_g = \frac{0.065\rho_g}{\rho_l - \rho_g} \frac{u_g - u_l}{g\bar{h}_g cos\theta}, \quad K_l = 10\sqrt{\frac{\rho_g}{\rho_l}} \left| \frac{u_g - u_l}{u_l} \right|, \tag{11}$$

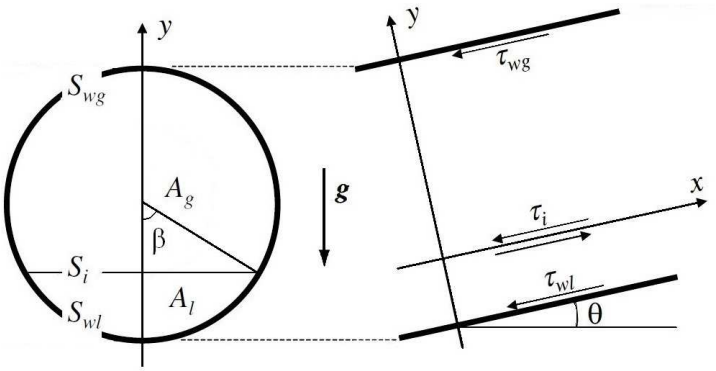

Figure 1: Schematic diagram of geometry.

in case of wavy interface.

Comparing the code here presented with the original one by Ferrari et al. [5], several modifications are applied in the computation of shear stresses at the wall and at the interface. This calculation now requires the parameters R_j and K_j, which are introduced in the corrected hydraulic diameter

$$D_{ej} = \frac{4A_j}{S_{wj}} \left(\frac{S_{wj}}{S_{wj} + S_i} \right)^{F(R_j, K_j)}, \tag{12}$$

as proposed in [4], where the wetted perimeter S_{wl} and S_{wg} and the interface perimeter S_i are shown in Fig. 1. The corrected hydraulic diameter is employed to compute the Reynolds number

$$Re_j = |u_j| \frac{\rho_j}{\mu_j} D_{ej}, \tag{13}$$

which is then used to obtain the friction factor f_j by the Colebrook-White interpolation

$$\frac{1}{\sqrt{f_j}} = -2\log_{10}\left(\frac{2.51}{Re_j \sqrt{f_j}} + \frac{k_s}{3.7D} \right) \tag{14}$$

in the case of turbulent flow, and

$$f_j = \frac{64}{Re_j} \tag{15}$$

in the case of laminar flow. In this work, both smooth and rough flows can be described thanks to the sand roughness k_s.

Finally, the gas shear stress at wall is computed as

$$\tau_{wg} = \frac{f_g}{4} \frac{\rho_g |u_g| u_g}{2}, \tag{16}$$

and the value of τ_i and τ_{wl} are computed by knowing τ_{wg}, R_g and R_l.

3. Numerical method

The numerical resolution of the modified five-equation model, Eqs. (1) - (5), is largely based on the one proposed by Ferrari et al. [5], in which the finite volume method with an explicit first order time discretisation is adopted. The Riemann problem at cell interface is solved by a Roe solver and numerical fluxes between cells are computed with the addition of a high resolution correction, obtaining second order accuracy in space. At each numerical iteration, the system of Eqs. (1) - (5) is solved in two consecutive substeps: first, the solution of the left-hand side of Eqs. (1) - (5), which represents the hyperbolic part of the system, is computed by the Roe linearisation proposed in [5] and in [9]; then, the source terms on the right-hand side of Eqs. (1) - (5) are added to the numerical solution, obtaining the new updated values of the set of variables for the following numerical step. In this second substep, the source term of the advection equation – Eq. (1) – is taken into account by an instantaneous pressure relaxation process, widely described in [5] and in [9], which requires the solution of a second degree equation: the gas volume fraction α_g is modified to restore pressure equality at the interface between liquid and gas phases. As mentioned in Sections 1 and 2, this pressure relaxation process ensures the possibility to account for surface tension effects; however, Ferrari et al. [5] showed that, almost in case of water-air flows in little or medium-size pipes, this addition has a negligible effect on results: therefore, in our applications presented in Section 4, surface tension is disregarded.
In the present work, the numerical solution of the hyperbolic part of the system of Eqs. (1) - (5) has been modified to account for shape factors that affects the eigenstructure of the system, see Section 2 and Appendix A, and, in particular, the formulation of matrices that appear in the Roe linearisation process.

Regarding the computation of velocity profiles, see Section 2, the value of the parameter R_g is computed in every computational cell and at every time step by a root search algorithm, imposing the equality of gas and liquid velocity in the y direction at the interface, while computing the shear stresses. Once that R_g is known, it is possible to obtain the velocity profile in the cross-sectional direction and, by a numerical integration, the shape factors value, which will be inserted in the Roe matrix in the following time step (at the beginning of a simulation, the shape factors are initialised equal to 1). The algorithm to obtain the value of R_g can be summarised as

1. compute shear stress between wall and gas phase τ_{wg}, knowing gas volume fraction, gas velocity and gas density;
2. compute shear stress at interface and between wall and liquid phase with relations $\tau_i = R_g \tau_{wg}$ and $\tau_{wl} = \tau_i / R_l$;
3. compute liquid and gas velocity at interface with Eq. (8);
4. compute R_g, τ_i and τ_{wl} in an iterative way until the no-slip condition at the interface is satisfied, i.e. the difference between gas and liquid velocity at the interface is lower than a prescribed tolerance.

Moreover, Ferrari et al. [5] developed a criterion to capture the transition from two-phase to single phase flow, which takes place as a slug emerges and grows: this method consists in setting gradually to zero the gas velocity when the gas volume fraction drops in a certain threshold interval (i.e. the gas momentum equation is gradually turned off); the values of the extremities of the threshold interval are very low, in the

range $3 \div 8 \cdot 10^{-3}$. In this work, a special treatment to handle the shape factors and velocity profile computation inside the slug body has been added to the existing transition criterion: this updated method prescribes that, when a slug forms, the shape factor of the gas phase is no longer computed, since it is no more required in the calculation concerning the gas momentum balance equation. On the other hand, regarding the liquid phase, we prescribe that the velocity profile inside the slug body follows the relation proposed by Biberg [4] in the case of Poiseuille-type flow: although this kind of flow is normally laminar, thanks to the turbulent viscosity employed in the computations, see Section 2, we obtain a turbulent shaped profile.

Finally, to allow the correct capture of the physical behaviour of slugs along the pipe, all simulations presented in next Section are performed choosing a spatial discretisation characterized by a cell interval about $0.5 \div 1 \cdot D$, where D is the internal diameter of the pipe. As consequence, to ensure a not too high value for the Courant-Friedrichs-Lewy condition, defined as

$$CFL = \frac{\Delta t}{\Delta x}|\lambda_{max}|, \tag{17}$$

the time step in all simulations is fixed to $\Delta t = 10^{-5}\ s$, since the maximum eigenvalue is approximately $10^3\ m/s$ (for further information on the eigenvalues, see Appendix A).

4. Results

In this Section results are presented: velocity profiles are analysed first in stratified flow conditions, Section 4.1, and, then, during initiation and development of slug flow regime, Section 4.2.

4.1. Stratified flow

In this Section, the computed cross-sectional velocity profiles in stratified flow conditions will be validated against the experimental measurements performed by Ayati et al. [6]: the geometry adopted in the experiments consists in a horizontal 31 m long PVC pipe, with an internal diameter $D = 0.1\ m$; the fluids used in the test cases are water and air, whose density are, respectively, 997 kg/m^3 and 1.2 kg/m^3.

Concerning the numerical simulations, the space discretisation consists in 620 cells, leading to a $\Delta x = D/2$, with a corresponding CFL

$$CFL = \frac{\Delta t}{\Delta x}|\lambda_{max}| \approx 0.2. \tag{18}$$

We perform four comparisons, with four different couples of superficial velocities, which are reported in Table 1: two of the chosen configurations are characterized by a smooth sub-regime and two by a 2D waves sub-regime, as observed by Ayati et al. [6]. In the case of smooth sub-regime (and therefore smooth interface), in our numerical simulations we adopt the relation for K_f shown in Eq. (10), while in case of 2D waves, Eq. (11) is employed. The PVC pipe roughness, required in Eq. (14), is set to the representative value of $5 \cdot 10^{-3}\ mm$, since the actual value is not reported in [6].

Ayati et al. [6] perform the PIV measurements in a vertical plane located at $260D$ downstream from inlet. Therefore, our numerical results are extracted at the same position along the pipe.

Table 1: Observed flow regimes and numerically computed shape factors for each couple of superficial velocities.

u_{ls} $[m/s]$	u_{gs} $[m/s]$	Sub-regime	γ_l	γ_g
0.08	1.09	Smooth	1.10	1.03
0.08	1.27	Smooth	1.09	1.04
0.10	2.03	2D waves	1.09	1.04
0.10	2.29	2D waves	1.10	1.04

Figs. 2 and 3 compare the experimental results with the numerical ones: the shapes of the computed velocity profiles are in good agreement with the experimental one (the experimental profiles present some discontinuities because of strong background reflections or restricted optical access in proximity of the interface, see [6]). In the case of smooth regime, there is a small discrepancy in the velocity magnitude: this can be due to the fact that the numerical code predicts an equilibrium value of the liquid volume fraction slightly higher than the one observed in the experiments: therefore, the flow section for the gas phase is smaller and the velocity at the nose of the profile is higher, while the opposite happens for the liquid phase, whose velocity magnitude of the flat profile is slightly lower than the observed one.

In Table 1 the computed shape factors for gas and liquid phase are reported.

4.2. Slug flow

For the numerical simulations in slug conditions, the adopted geometry consists in a 36 m long pipe, with and internal diameter $D = 0.078$ m [1]; in this case we adopt $\Delta x = 0.577D$ and $CFL = 0.22$. The liquid and gas superficial velocities are, respectively, $u_{ls} = 1.5m/s$ and $u_{gs} = 2.0m/s$; the simulated fluids are again water and air.

Figure 4 reports the qualitative behaviour of the velocity profiles before (top) and after (bottom) the slug development. It is possible to observe that, before slug formation, a wave forms and velocity profiles adapt themselves as the liquid volume fraction changes along the pipe; then, this wave grows to form a slug and a turbulent Poiseuille-type profile can be observed inside the slug body.

Dukler et al. [7] formulated the one-seventh power law to describe the velocity profile in the slug body

$$v_l = v_0 \left(\frac{y}{\delta} \right)^{1/7}. \tag{19}$$

and, later, their assumptions were supported by experimental observations, see [8]. In Fig. 5 the computed profile in a slug body is compared against the one-seventh power law, which was calculated with $\delta = D/2$, since the profile is assumed to be fully developed and the thickness of the boundary layer δ is equal to the pipe radius, see [8]. The velocity v_0 is obtained summing the gas and liquid superficial velocities, i.e. $v_0 = u_{ls} + u_{gs} = 3.5$ m/s: this choice is justified by the fact that the centerline velocity v_0 is very close to the slug velocity, see [15]. As can be seen, the computed velocity profile is not far from the one-seventh power law; the shape factor in the slug body is in the range $1.02 \div 1.04$.

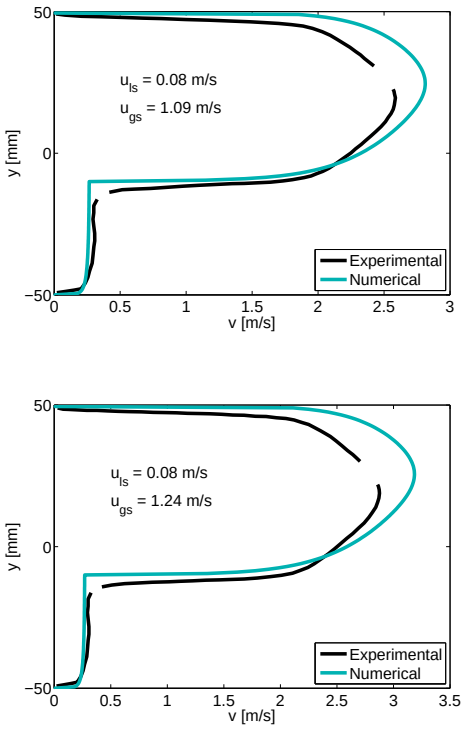

Figure 2: Comparison of the experimental and the numerical velocity profiles at $x = 260D$. Smooth sub-regime.

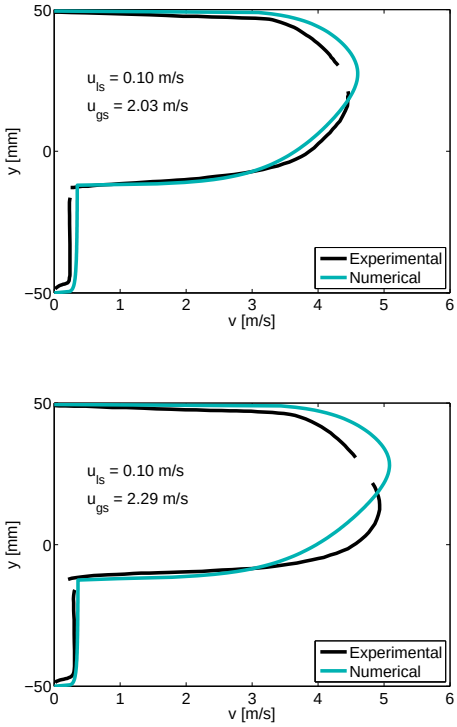

Figure 3: Comparison of the experimental and the numerical velocity profiles at $x = 260D$. 2D waves sub-regime.

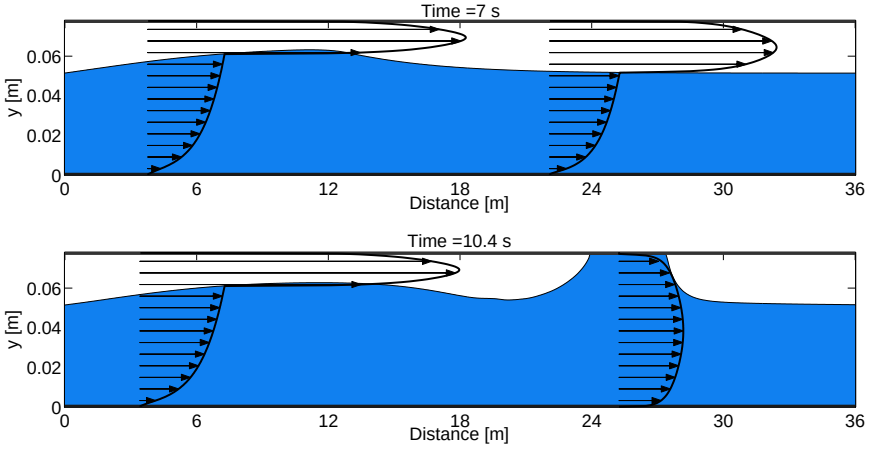

Figure 4: Qualitative behaviour of computed velocity profiles along the pipe before (top) and after (bottom) slug formation.

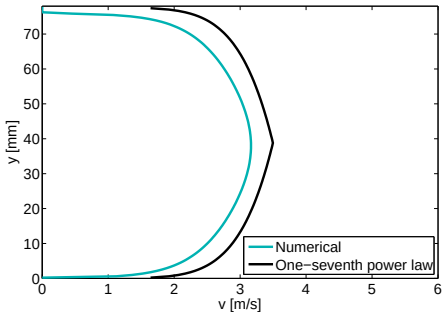

Figure 5: Slug flow case. Comparison of the one-seventh power law velocity profile against the computed one.

5. Conclusion

In this work, a one-dimensional, transient, hyperbolic, five-equation two-fluid model accounting for cross-sectional velocity distribution has been presented. Starting from an existing numerical code by Ferrari et al. [5] possessing advantageous characteristics, the model has been modified to account for the shape of the velocity profiles by inserting the γ factors in the gas and liquid momentum balance equations; the inclusion of these correction coefficients modifies the five-equation system eigenstructure, whose explicit form has been computed since we aimed at using the Roe linearisation in the numerical resolution. A pre-integrated model [4] has been embodied in the numerical code, to compute shear stresses at wall and at interface and to obtain a consistent description of the cross-sectional velocity distribution.

Numerical results both in stratified and in slug flow regime have been presented. The computed velocity profiles in smooth and wavy stratified regime were compared against experimental measurements, showing good agreement. Moreover, a method to compute the velocity profile during the transition from two-phase to single phase flow (which occurs during slug formation) has been developed; the computed velocity distribution in the liquid phase blocks (i.e. a slug) follows quite accurately the one-seventh power law profile, which has been experimentally observed to occur in the slug body.

Appendix A. Comparison of the eigenstructure with and without the inclusion of the shape factors in the model

The eigenvalues and the eigenvectors of the five-equation system matrix with and without the shape factor inclusion in the model are here reported, to show how deeply the description of the velocity profiles affects the eigenstructure of the five-equation system.

First, the eigenvalues of the five-equation system not accounting for the shape factors,

computed by Ferrari et al. [5], are

$$\boldsymbol{\lambda} = \begin{bmatrix} u_\mathrm{i} \\ u_g - c_g \\ u_g + c_g \\ u_l - c_l \\ u_l + c_l \end{bmatrix}, \tag{A.1}$$

while the ones modified in the present work, accounting for shape factors in the gas and liquid momentum balance equations, are

$$\boldsymbol{\lambda} = \begin{bmatrix} u_\mathrm{i} \\ \frac{u_g}{2}(1+\gamma_g) - \frac{\sqrt{4c_g^2+[u_g(\gamma_g-1)]^2}}{2} \\ \frac{u_g}{2}(1+\gamma_g) + \frac{\sqrt{4c_g^2+[u_g(\gamma_g-1)]^2}}{2} \\ \frac{u_l}{2}(1+\gamma_l) - \frac{\sqrt{4c_l^2+[u_l(\gamma_l-1)]^2}}{2} \\ \frac{u_l}{2}(1+\gamma_l) + \frac{\sqrt{4c_l^2+[u_l(\gamma_l-1)]^2}}{2} \end{bmatrix}, \tag{A.2}$$

where $c_g = 316\ m/s$ and $c_l = 1000\ m/s$ are the speed of sound respectively for gas and liquid phase, which derive from the equation of state formulation, see [5] for details.

The eigenvectors of the five-equation system matrix without the shape factors are

$$\mathbf{R} = \begin{bmatrix} 1 & 0 & 0 & 0 & 0 \\ -\frac{c_g^2\rho_g+\alpha_g\rho_g\zeta}{[(u_g-u_\mathrm{i})^2-c_g^2]} & 1 & 1 & 0 & 0 \\ -\frac{c_g^2\rho_g+\alpha_g\rho_g\zeta}{[(u_g-u_\mathrm{i})^2-c_g^2]}u_\mathrm{i} & u_g - c_g & u_g + c_g & 0 & 0 \\ \frac{c_l^2\rho_l-\alpha_l\rho_l\zeta}{[(u_l-u_\mathrm{i})^2-c_l^2]} & 0 & 0 & 1 & 1 \\ \frac{c_l^2\rho_l-\alpha_l\rho_l\zeta}{[(u_l-u_\mathrm{i})^2-c_l^2]}u_\mathrm{i} & 0 & 0 & u_l - c_l & u_l + c_l \end{bmatrix}, \tag{A.3}$$

where $\zeta = -\frac{\pi D g \cos\theta}{4\sin(\beta)}$; the eigenvectors of the system matrix including γ factors are

$$\mathbf{R} = \begin{bmatrix} 1 & 0 & 0 & 0 & 0 \\ r_{21} & 1 & 1 & 0 & 0 \\ r_{31} & \frac{\gamma_g u_g^2 - c_g^2}{\lambda_3} & \frac{\gamma_g u_g^2 - c_g^2}{\lambda_2} & 0 & 0 \\ r_{41} & 0 & 0 & 1 & 1 \\ r_{51} & 0 & 0 & \frac{\gamma_l u_l^2 - c_l^2}{\lambda_5} & \frac{\gamma_l u_l^2 - c_l^2}{\lambda_4} \end{bmatrix}, \tag{A.4}$$

with

$$\begin{aligned} r_{21} &= -\frac{c_g^2\rho_g + \alpha_g\rho_g\zeta}{[\gamma_g u_g^2 - u_g u_\mathrm{i}(1+\gamma_g) + u_\mathrm{i}^2 - c_g^2]}, \\ r_{31} &= -\frac{c_g^2\rho_g + \alpha_g\rho_g\zeta}{[\gamma_g u_g^2 - u_g u_\mathrm{i}(1+\gamma_g) + u_\mathrm{i}^2 - c_g^2]}u_\mathrm{i}, \\ r_{41} &= \frac{c_l^2\rho_l - \alpha_l\rho_l\zeta}{[\gamma_l u_l^2 - u_l u_\mathrm{i}(1+\gamma_l) + u_\mathrm{i}^2 - c_l^2]}, \\ r_{51} &= \frac{c_l^2\rho_l - \alpha_l\rho_l\zeta}{[\gamma_l u_l^2 - u_l u_\mathrm{i}(1+\gamma_l) + u_\mathrm{i}^2 - c_l^2]}u_\mathrm{i}. \end{aligned} \tag{A.5}$$

It is possible to observe that, when in Eqs. (A.2) and (A.4) γ_g and γ_l are unitary, the expressions without the shape factor of Eqs. (A.1) and (A.3) are recovered. Therefore, the eigenstructure of the model including shape factors can be seen as an extension of the one presented in [5] and, conversely, the eigenstructure of the system matrix without shape factor can be seen as a particular case of the one obtained in the present work.

Appendix A.1. On the hyperbolicity of the five-equation system

A model is defined as be well-posed if it satisfies the existence and uniqueness of its solution and the continuous dependence on the data. The requirement on the continuous dependence of data is necessary to ensure that small changes in initial data correspond to small changes in the solution: for a system of partial differential equations, this property is strongly related to hyperbolicity, as shown by Prosperetti and Tryggvason [16].

Ferrari et al. [5] proved the hyperbolicity of the their five-equation system using the method suggested in [9]and in [16]: a system of partial differential equation is hyperbolic if the system matrix eigenvalues are real and its eigenvectors form a basis of the vector space of the solution of dimension m, which is the number of equations appearing in the PDE system. They observed that the five-equation system is hyperbolic if the transonic condition, i.e. at high flow speed $u_j \pm c_j = u_i$, is avoided, and this condition is always satisfied since low-speed flow are considered.

A similar analysis can be made on the five-equation system modified with the shape factors inclusion: the eigenvalues A.2 are always real (since the terms under the square root are always positive) and the eigenvectors are linearly independent except for the transonic condition, rewritten in terms of the shape factors, $c_j = \sqrt{\gamma_j u_j^2 - u_j u_i (1 + \gamma_j) + u_i^2}$. Since, we deal only with low-speed flow and the simulation conditions are always far from the transonic difficulty, we can assert that the five-equation system modified with the shape factor maintains the hyperbolicity properties valid for the five-equation system non accounting for the shape factors.

Appendix B. Further equations adopted in the model

In this Appendix, we report the equations developed by Biberg [4] and adopted in the presented model.

Δ_j and C_j, adopted in Eq. (8), are (the subscript j has been removed for clarity)

$$\begin{aligned}\Delta = &\ln(1-Y) + \frac{(K^3+R^3)\ln(Y+K(1-Y))}{|R|^{5/2}-K^3} \\ &+ \frac{(R+\sqrt{|R|})\sqrt[3]{|R|}ln(Y+|R|^{5/6}(1-Y))}{3(K-|R|^{5/6})} \\ &- (R+\sqrt{|R|})(K+2|R|^{5/6})|R|^{5/6}\sqrt[3]{|R|} \\ &\cdot \frac{\ln Y^2-(1-Y)(Y-(1-Y)|R|^{5/6})}{6(K^2+|R|^{5/6}K+|R|^{5/3})} \\ &+ \frac{K(R+\sqrt{|R|})\sqrt[3]{|R|}}{\sqrt{3}(K^2+|R|^{5/6}K+|R|^{5/3})} \\ &\cdot \tan^{-1}\left(\frac{2(Y-1)|R|^{5/3}+(2Y-1)|R|^{5/6}+2Y}{\sqrt{3}|R|^{5/6}}\right)\end{aligned} \tag{B.1}$$

and

$$C = C^1 + sgn(\tau_w)\frac{u^*}{\kappa}\psi, \tag{B.2}$$

where

$$C^1 = sgn(\tau_w)\frac{u^*}{\kappa}\left(\ln\left(\frac{h}{k_s}\right)+A\kappa\right), \tag{B.3}$$

and

$$\psi = -\frac{K(R+\sqrt{|R|})\sqrt[3]{|R|}}{\sqrt{3}(K^2+|R|^{5/6}K+|R|^{5/3})}\tan^{-1}\left(\frac{1+2/|R|^{5/6}}{\sqrt{3}}\right). \tag{B.4}$$

The exponent $F(R_j, K_j)$ reported in Eq. (12) is (the subscript j has been removed for clarity)

$$F(R,K) = \frac{\Lambda+\psi}{\Lambda^P}, \tag{B.5}$$

where

$$\begin{aligned}\Lambda = &\frac{5(R+\sqrt{|R|})(|R|^{5/2}+K^2+K)R^2\ln(|R|)}{6(K^3-|R|^{5/2})(|R|^{5/2}-1)} \\ &- \frac{K(K^3+R^3)\ln(K)}{(K-1)(K^3-|R|^{5/2})} \\ &+ \frac{(R+\sqrt{|R|})\sqrt[3]{|R|}}{\sqrt{3}(|R|^{5/3}+|R|^{5/6}+1)(K^2+K|R|^{5/6}+|R|^{5/3})} \\ &\cdot\left((K-|R|^{5/3})\tan^{-1}\left(\frac{1+2/|R|^{5/6}}{\sqrt{3}}\right)\right. \\ &\left.-(K+(K+1)|R|^{5/6})|R|^{5/6}\tan^{-1}\left(\frac{2|R|^{5/6}+1}{\sqrt{3}}\right)\right),\end{aligned} \tag{B.6}$$

and

$$\Lambda^P = -\frac{2}{27}(2\sqrt{3}+9). \tag{B.7}$$

References

[1] R. I. Issa, M. H. W. Kempf, Simulation of slug flow in horizontal and nearly horizontal pipes with the two-fluid model, International Journal of Multiphase Flow 29 (2003) 69 – 95.

[2] F. Renault, A lagrangian slug capturing scheme for gas-liquid flows in pipes, Vol. Phd Thesis 2005, NTNU, Trondheim, Norway, 2007.

[3] M. Bonizzi, P. Andreussi, S. Banerjee, Flow regime independent, high resolution multi-field modelling of near-horizontal gas-liquid flows in pipelines, International Journal of Multiphase Flow 35 (2009) 34 – 46.

[4] D. Biberg, A mathematical model for two-phase stratified turbulent duct flow, Multiphase Science and Technology 19 (2007) 1 – 48.

[5] M. Ferrari, A. Bonzanini, P. Poesio, A five-equation, transient, hyperbolic, one-dimensional model for slug capturing in pipes, International Journal for Numerical Method in Fluids (2017).

[6] A. Ayati, J. Kolaas, G. Johnson, Combined simultaneous two-phase piv and interface elevation measurements in stratified gas/liquid pipe flow, International Journal of Multiphase Flow 74 (2015) 45 – 58.

[7] A. E. Dukler, D. Moalem Maron, N. Brauner, A physical model for predicting the minumum stable slug length, Chemical Engineering Science 40 (1985) 1379 – 1385.

[8] M. Gopal, W. P. Jepson, Development of digital image analysis techniques for the study of velocity and void profiles in slug flow., International Journal of Multiphase Flow 23 (1997) 945 – 965.

[9] S. T. Munkejord, I. R. Gran, Modelling and numerical methods for two-phase flow, Vol. Phd Thesis 2005, NTNU, Trondheim, Norway, VDM Verlag Dr. Müller Aktiengesell & Co. KG, 2009.

[10] R. Saurel, R. Abgrall, A multiphase Godunov method for compressible multifluid and multiphase flow, Journal of Computational Physics 150 (2) (1999) 425–467.

[11] Y. Taitel, A. E. Dukler, A model for predicting flow regime transitions in horizontal and near horizontal gas-liquid flow, AIChE Journal 22 (1) (1976) 47–55.

[12] J. E. Kowalsky, Wall and interfacial shear stress in stratified flow in a horizontal pipe, AIChE Journal 33 (1987) 274–281.

[13] N. P. Hand, Gas-liquid co-current flow in a horizontal pipe, Ph.D. thesis, Queen's University Belfast, Belfast (January 1991).

[14] D. Picchi, S. Correra, P. Poesio, Flow pattern transition, pressure gradient, hold-up predictions in gas/non-newtonian power-law fluid stratified flow, International Journal of Multiphase Flow 63 (2014) 105 – 115.

[15] W. P. Jepson, Modelling the transition to slug flow in horizontal conduit, Canadian Journal of Chemical Engineering 67 (1989) 731 – 740.

[16] A. Prosperetti, G. Tryggvason, Computational Methods for Multiphase Flow, Cambridge University Press, 2007.